A generalized many-body expansion and a unified view of fragment-based methods in electronic structure theory

Ryan M. Richard and John M. Herbert[a)]
Department of Chemistry and Biochemistry, The Ohio State University, Columbus, Ohio 43210, USA

(Received 15 May 2012; accepted 24 July 2012; published online 13 August 2012)

Fragment-based quantum chemistry methods are a promising route towards massively parallel electronic structure calculations in large systems. Unfortunately, the literature on this topic consists of a bewildering array of different methods, with no clear guiding principles to choose amongst them. Here, we introduce a conceptual framework that unifies many of these ostensibly disparate approaches. The common framework is based upon an approximate supersystem energy formula for a collection of intersecting (i.e., overlapping) fragments. This formula generalizes the traditional many-body expansion to cases where the "bodies" (fragments) share some nuclei in common, and reduces to the traditional many-body expansion for non-overlapping fragments. We illustrate how numerous fragment-based methods fit within this framework. Preliminary applications to molecular and ionic clusters suggest that two-body methods in which dimers are constructed from intersecting fragments may be a route to achieve very high accuracy in fragment-based calculations. [http://dx.doi.org/10.1063/1.4742816]

I. INTRODUCTION

The cost of *ab initio* electronic structure calculations increases steeply as a function of both system size (number of atoms, N_A) and also one-particle basis size (number of basis functions per atom, N_B). The cost can be characterized as $\mathcal{O}(N_A^a N_B^b)$, where typically $b = 2$–4 and $a \geq 3$, depending upon the *ab initio* method in question. Fragment-based methods[1] represent a promising path toward reducing the computational scaling with respect to N_A. In such methods, the energy of a large molecule or cluster is decomposed in terms of the energies of a collection of smaller subsystems, each of which is assumed to be representative of the local electronic environment. This idea has an undeniable intuitive appeal, as chemists are accustomed to reasoning in terms of functional groups, localized orbitals, and electron pairs, and is consistent with Kohn's notion of the "nearsightedness" of electronic matter.[2,3] If the N_A-atom system can be decomposed into N_F smaller fragments (each of size n_A, say), then the computational scaling for a fixed basis set is reduced from $\mathcal{O}(N_A^a)$ to $N_F \times \mathcal{O}(n_A^a)$. This is potentially a huge speedup, even more so because the N_F smaller calculations are completely independent and therefore qualify as "embarrassingly parallelizable."

Of course, the proverbial devil lies in the as-yet-unspecified details. While these ideas have been around for a long time,[4–6] the past decade has seen a flurry of activity resulting in a tremendous variety of fragment-based quantum chemistry methods that seek better approximations to the total system energy. (See Ref. 1 for a lengthy review, albeit one that still falls short of an exhaustive list of fragment-based methods.) Relationships between these methods are not always clear,[7] and one aim of the present work is to develop a common theoretical framework to describe this plethora of methods.

Several recent papers have attempted to classify extant fragment methods within a systematic framework.[1,7,8] A recent review[1] categorizes these approaches as either "one-step" methods, in which the property of interest (almost always the energy) is computed directly from fragment calculations; or else "two-step" methods, wherein the fragment calculations are first used to construct the supersystem density matrix, which is then used to compute supersystem properties. (For one-step methods, properties other than the total energy must be cast as energy derivatives.[9]) Two-step methods are not considered here. Gordon *et al.*[1] further distinguish between three different types of fragmentation schemes:

- those in which only monomers are used;
- those in which unions of two or more fragments are used; and
- those in which monomers intersect with one another.

One result of the present work is the recognition that non-intersecting fragments can be handled as a special case of intersecting fragments.

Mayhall and Raghavachari[8] recently provided an important step toward unifying (or at least, classifying) existing fragment methods, by showing how one can specify such methods in an elemental manner. According to their classification scheme, one must specify:

(1) a method for defining "groups" of atoms,
(2) a method for fragmenting the supersystem, and
(3) selection of an appropriate energy expression in terms of the fragment energies.

These authors furthermore proposed what they termed a "molecules-in-molecules" approach, in which the supersystem energy is expressed using an ONIOM-like equation,[10,11]

a)Electronic mail: herbert@chemistry.ohio-state.edu.

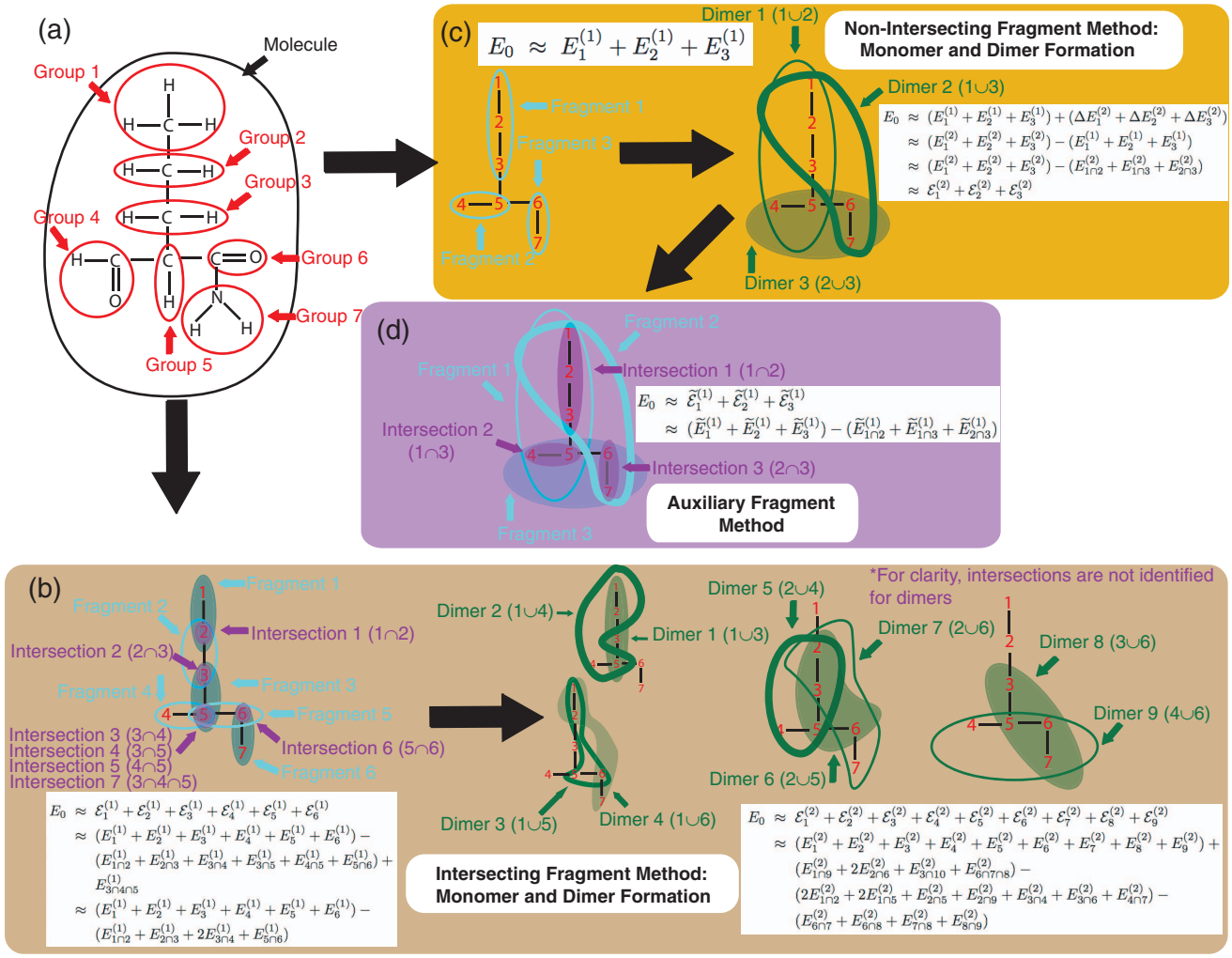

FIG. 1. An illustrated example of the nomenclature used in this study. Panel (a) defines groups for a particular molecule. Panel (b) illustrates fragmentation of the molecule and dimer formation, using fragments that are allowed to intersect. Panel (c) depicts a particular fragmentation using non-intersecting monomers. Panel (d) illustrates the use of auxiliary monomers. Consult the text for further explanation.

such that different fragments may be described at different levels of theory. Although fragment-based methods, by their very definition, will probably never satisfy Pople's definition of a *theoretical model chemistry*,[12] the elemental approach in Ref. 8 brings us much closer to a systematic hierarchy of fragment-based methods.

Restricting our attention to one-step methods in which the supersystem energy is computed directly from subsystem (fragment) energy calculations, our own survey of the literature suggests two distinct paradigms for decomposing a system into fragments. The first—and more common—approach is to construct fragments by partitioning the nuclei into disjoint subsets. The total system energy can be determined from the subsystem energies by means of a many-body expansion (MBE),[1,13,14] truncated at some finite order. Higher-order terms are sometimes included by performing a full supersystem calculation at a lower level of theory,[15–23] which might be a force field.[14–17] (Hybrid methods of this sort fit within the ONIOM-type formalism mentioned above.) As an alternative to using disjoint fragments, one might allow intersections between the subsets of nuclei, such that a given nucleus might belong to more than one fragment. The latter approach precludes a straightforward summation of the fragment energies, and a variety of energy formulas have been suggested in the case of intersecting fragments.[24–26]

The purpose of this work is to unify these two seemingly disparate notions under a common energy formula, such that various fragment methods can be viewed as different truncations of—or approximations to—a "master" energy expression. This simplifies element (3) in the prescription above, by providing a universal formula to which approximations can be made. We will then compare the results of several different truncation schemes, some of which correspond to previously proposed fragment methods but some of which are new.

II. THEORY

A. Nomenclature

The goal of this work is to systematize numerous fragment-based methods, thus we require a systematic notation. Figure 1 introduces this notation by means of a specific example. We define the entire (super)system to be the molecule, irrespective of whether it is actually a single large molecule or a cluster of smaller molecules. Most

fragmentation algorithms then partition the molecule into a set of *groups*. We define a group to be collection of nuclei that are never separated, perhaps because they represent some chemical moiety characterized by significant electron delocalization. Often, groups are created by severing all single covalent bonds between heavy atoms,[8,24] which is the procedure that is followed in the example of Fig. 1(a). One then selects a *fragmentation method* to assign groups to fragments. Each fragment consists of a specified set of groups. These fragments, which will also be called *monomers* (for reasons that should become clear later on) represent the basic building blocks of the calculation.

It was suggested by Suárez *et al.*[7] that all fragment-based approaches could be classified according to whether they employ intersecting or non-intersecting fragments, a distinction that is paramount to the forthcoming discussion. Two fragments are said to intersect if they contain a common group, that is, if their intersection as sets is not empty. The first diagram in Fig. 1(b) illustrates one particular way in which a set of intersecting fragments might be formed, and the intersections are labeled using the notation of set theory. Figure 1(c) depicts an alternative fragmentation scheme in which the fragments do not intersect. (Automated criteria for constructing fragments will be discussed in Sec. II E; the choices in Fig. 1 are intended purely for illustrative purposes.)

In both Figs. 1(b) and 1(c), fragmentation severs covalent bonds; in order to restore the correct valencies, these severed bonds must be capped. We define a *capping method* as an algorithm to determine the cap and its properties, such as its charge and position relative to the valence that it is intended to saturate. Most often the cap is a hydrogen atom and is simply placed at the location of the "missing" atom involved in the covalent bond. (One might worry about an anomalously long bond length to the hydrogen atom. This point has been addressed in the literature,[24] and is discussed in Sec. II E.) The sum of the fragment energies constitutes the "one-body" energy that represents the first approximation to the ground-state energy. Note that if fragments A and B intersect ($A \cap B \neq \emptyset$), then it will be necessary to cap the fragment $A \cap B$, as the energy of $A \cap B$ will appear in the generalized many-body expansion (GMBE) that is introduced in Sec. II D.

B. Many-body expansion

Having introduced the notation (if not the algorithms) for elements (1) and (2) in the classification scheme[8] discussed in Sec. I, we next consider element (3), the energy formula. For non-intersecting fragments that do not cut across covalent bonds, it has long been recognized that the *exact* ground-state energy, E, can be expressed in terms of the energies of monomers, dimers, trimers, etc., by means of the MBE. The most conceptually straightforward way to write the MBE is[13]

$$E = \sum_{I=1}^{N} E_I^{(1)} + \sum_{\substack{I,\,J \\ (I<J)}}^{N} \left(E_{IJ}^{(2)} - E_I^{(1)} - E_J^{(1)}\right) + \sum_{\substack{I,\,J,\,K \\ (I<J<K)}}^{N} \Big[E_{IJK}^{(3)} - E_I^{(1)} - E_J^{(1)} - E_K^{(1)} - \left(E_{IJ}^{(2)} - E_I^{(1)} - E_J^{(1)}\right) - \left(E_{IK}^{(2)} - E_I^{(1)} - E_K^{(1)}\right) - \left(E_{JK}^{(2)} - E_J^{(1)} - E_K^{(1)}\right)\Big] + \cdots . \quad (1)$$

Here, $E_I^{(1)}$ is the energy of the Ith monomer and $E_{IJ}^{(2)}$ represents the energy of the dimer constructed from monomers I and J, etc.

At each order in the MBE, one subtracts out lower-order interactions to avoid overcounting, and for our purposes it will be more convenient to rewrite Eq. (1) in terms of two-body and higher-order energy corrections,[15] such as

$$\Delta E_{IJ}^{(2)} = E_{IJ}^{(2)} - E_I^{(1)} - E_J^{(1)}. \quad (2)$$

The various energy corrections $E_I^{(1)}$, $\Delta E_{IJ}^{(2)}$, $\Delta E_{IJK}^{(3)}, \ldots$ may be computed at different levels of theory.[14–19,27]

For brevity, we will forgo the "IJ" notation in Eqs. (1) and (2) in favor of a single index that runs over all

$${}_N C_n = \frac{N!}{n!(N-n)!} \quad (3)$$

combinations of n fragments, and rewrite the MBE in Eq. (1) as

$$E = \sum_{\alpha=1}^{N} E_\alpha^{(1)} + \sum_{\alpha=1}^{{}_N C_2} \Delta E_\alpha^{(2)} + \sum_{\alpha=1}^{{}_N C_3} \Delta E_\alpha^{(3)} + \cdots . \quad (4)$$

We define $E_\alpha^{(n)}$ to be the energy of the αth "n-mer" constructed from a union of n different fragments, where $\alpha = 1, 2, \ldots, {}_N C_n$ indexes the unique combinations of n fragments. Then $\Delta E_\alpha^{(n)}$ is analogous to Eq. (2) and subtracts out the appropriate lower-order interactions involving these fragments. A recursive expression for these energy corrections is

$$\Delta E_\alpha^{(n)} = E_\alpha^{(n)} - \sum_{\beta=1}^{{}_n C_{n-1}} \Delta E_\beta^{(n-1)} - \sum_{\gamma=1}^{{}_n C_{n-2}} \Delta E_\gamma^{(n-2)} - \cdots - \sum_{\omega=1}^{n} E_\omega^{(1)}. \quad (5)$$

The summations in this equation extend only over the fragments that constitute the αth n-mer. For example, if $n = 3$ and we consider the trimer consisting of fragments a, b, and c, then the index β in Eq. (5) runs over the ${}_3C_2$ dimers $a \cup b$, $a \cup c$, and $b \cup c$.

The recursive definition in Eq. (5) suggests that $\Delta E_\alpha^{(1)} = E_\alpha^{(1)}$. This makes sense, in the context of Eq. (4), given that the sum of one-body energies constitutes a first approximation to the supersystem energy, E. More generally, we can rewrite Eq. (4) as

$$E = \sum_{n=1}^{N} \left(\sum_{\alpha=1}^{{}_N C_n} \Delta E_\alpha^{(n)} \right). \quad (6)$$

This represents a very concise expression of the MBE, which we will attempt to generalize (in Sec. II D) to cases where the fragments intersect. For non-intersecting fragments, Eq. (6) is a formally exact expression that in practice would be truncated at some value of $n < N$. Neglecting terms in

Eq. (6) for which $n > m$ affords an m-body approximation, $E^{(m)}$, to the total energy. A formula for $E^{(m)}$ can be expressed recursively, in terms of the lower-order k-body energy expressions, $E^{(k)}$:[28]

$$E^{(m)} = \sum_{\alpha=1}^{{}_N C_m} E_\alpha^{(m)} - \sum_{k=1}^{m-1} \left[\frac{(N-k)!}{(N-m)!(m-k)!} \right] E^{(k)}. \quad (7)$$

Note that $E^{(1)}$ equals the sum of the monomer energies, hence Eq. (7) ultimately does provide a closed formula for $E^{(m)}$ in terms of the energies of k-mers of fragments (with $k \leq m$). The sum $E^{(1)} + E^{(2)} + E^{(3)} + \cdots$ is precisely the form of the MBE that is given in Eq. (1).

C. Intersecting fragments

Our goal is to develop a formula analogous to Eq. (7) that is valid in the case of intersecting fragments. To the best of our knowledge, it was recognized only recently[8] that existing fragment-based methods that employ intersecting fragments are essentially invoking the approximation

$$E \approx \sum_{\alpha=1}^{N} \mathcal{E}_\alpha^{(1)}, \quad (8)$$

where $\mathcal{E}_\alpha^{(1)}$ will be called the *intersection-corrected energy* for fragment α, and is defined by

$$\mathcal{E}_\alpha^{(1)} = E_\alpha^{(1)} - \sum_{\substack{\beta \\ (\beta > \alpha)}} E_{\alpha\cap\beta}^{(1)} + \sum_{\substack{\beta,\gamma \\ (\gamma > \beta > \alpha)}} E_{\alpha\cap\beta\cap\gamma}^{(1)} - \cdots . \quad (9)$$

In this expression, $E_{\alpha\cap\beta}^{(1)}$ denotes the energy of the subsystem constructed from the intersection of fragments α and β, and $E_{\alpha\cap\beta\cap\gamma}^{(1)}$ denotes the energy of a system construction from the intersection of three different fragments. (If construction of these intersections requires severing covalent bonds, then a method for capping severed valencies is required. This is discussed in Sec. II E.) Equation (9) has its origin in the set-theoretical principle of inclusion/exclusion (PIE), and we will argue in Sec. II D that the "intersection" terms ($E_{\alpha\cap\beta}^{(1)}$, etc.) prevent the overcounting of electron–electron and electron–nucleus interactions. As discussed below, the expansion naturally terminates when all of the intersections $\alpha \cap \beta \cap \cdots \cap \omega$ are empty.

The approximation defined in Eqs. (8) and (9) is equivalent to the energy expression used in the *cardinality-guided molecular tailoring approach* (CG-MTA).[25,29,30,60] Only recently was it recognized[8] that precisely the same expression is utilized in the *generalized energy-based fragmentation* (GEBF) approach,[26,31,32] another method that exploits intersecting fragments. This energy expression is also reminiscent of the formulas that are obtained by following the *systematic molecular fragmentation* (SMF) procedure.[24,33–35] However, we have implemented the SMF procedure and thereby confirmed that it generates only a limited subset of the intersections in Eq. (9) that are suggested by PIE. Rather than using set theory, the GEBF and SMF methods instead construct elaborate rules to avoid overcounting and thereby obtain the ± 1 coefficients that appear in Eq. (9), which may account for the delayed recognition of the similarities between these methods. In contrast, PIE provides a conceptually simple means to obtain the energy formula, once the molecular fragmentation scheme has been specified.

Unlike the traditional MBE for non-intersecting fragments, which is formally exact, Eq. (8) is fundamentally approximate, which begs the question of why one might wish to consider approaches based on intersecting fragments at all. Both approaches have potential strengths and weaknesses. For the traditional MBE in Eq. (6), one expects the corrections $\Delta E_\alpha^{(n)}$ to become smaller as n increases, so that the expansion might reasonably be truncated at fairly low order. Three-body expansions tend to be about an order-of-magnitude better approximations to E than are two-body expansions,[13] although this need not be the case in general. (See Ref. 22 for an example where a higher-order many-body approximation affords *less* accurate results. This particular example was analyzed in Ref. 15, where it is shown that error cancellation plays a pivotal role in the accuracy of these methods.) In any case, the potentially exact nature of MBE facilitates systematic convergence tests, which is an appealing characteristic that is lost in the intersecting-fragment expression of Eq. (8). On the other hand, Eq. (8) has a potential advantage in that it may include certain inter-monomer interactions already at the *one-body* level, depending on the nature of the fragmentation method, whereas such interactions do not appear in the conventional MBE until the two-body level.

As an example, consider the fragmentation scheme illustrated in Fig. 1(b), specifically, the fragments labeled 1, 2, and 3. All four groups contained within these three fragments are actually contained within the union $1 \cup 3$, and therefore application of the MBE does not require the existence of fragment 2 at all. In the absence of fragment 2, however, the interaction between *groups* 2 and 3 appears for the first time at the level of dimers (specifically, the dimer formed from the union of fragments 1 and 3). By including fragment 2, the interaction of groups 2 and 3 appears already at the one-body level. Although this requires an additional one-body calculation (on fragment 2), the benefit might conceivably outweigh the cost, given the steep scaling of quantum chemistry calculations with system size. In other words, a larger number of low-order n-body calculations, involving intersecting fragments, might be preferable to a smaller number of calculations where n is larger, if comparable accuracy can be obtained at reduced cost.

With these considerations in mind, it would be useful to have a means to include these inter-group interactions already in the one-body terms (by means of intersecting fragments), yet still have a systematic means of converging to the exact ground-state energy. To obtain such a method, we will generalize Eq. (8) by including two-body and higher-order terms, ultimately obtaining an approximation reminiscent of Eq. (7). This is taken up in Sec. II D, where we attempt to generalize the traditional MBE, Eq. (6), to encompass both intersecting and non-intersecting fragments.

D. Generalized many-body expansion

In this section we present a GMBE in the spirit of Eq. (7), except that it applies to both intersecting and non-intersecting monomers. For a collection of N monomers, we note that the MBE truncated at the n-body level is not exact except in the trivial case that $n = N$. The GMBE presented below has the same feature, but the logic behind this generalized expression is different.

1. Basic idea

The motivation for the GMBE is rooted in PIE, which is a theorem about the cardinality of sets. Let $S_1, S_2, \ldots, S_N$ be subsets of some set S; these subsets need not be disjoint. PIE states that the cardinality of S can be expressed as

$$\begin{aligned} |S| &= \sum_{i=1}^{N} |S_i| - \sum_{\substack{i,j \\ (i<j)}}^{N} |S_i \cap S_j| + \sum_{\substack{i,j,k \\ (i<j<k)}}^{N} |S_i \cap S_j \cap S_k| \\ &\quad - \cdots + (-1)^{N-1} |S_1 \cap S_2 \cap \cdots \cap S_N| \\ &= \sum_{n=1}^{N} (-1)^{n+1} \sum_{\substack{i_1, i_2, \ldots, i_n \\ (i_1 < i_2 < \cdots < i_n)}}^{n} |S_{i_1} \cap S_{i_1} \cap \cdots \cap S_{i_n}|. \end{aligned} \tag{10}$$

This expression is immediately reminiscent of the intersection-corrected energy defined in Eq. (9), but the connection between that equation and set theory is not obvious. The connection is the following: let S be the set of nuclei in the supersystem, and let $S_1, S_2, \ldots S_N$ be the subsets consisting of the nuclei contained in each fragment. We exploit the nuclei as means to keep track of the various Coulomb interactions that appear in the supersystem's electronic Hamiltonian. PIE, applied to the set of nuclei, *exactly* prevents us from overcounting (or undercounting) the nucleus–nucleus interactions, and we conjecture that this principle will *approximately* eliminate overcounting of the other interactions, insofar as the electrons are largely bound to the nuclei and any counting argument that are applicable to the nuclei may therefore be *approximately* applicable to the electrons.

The gist of this argument is that we will obtain the GMBE simply by replacing the cardinalities appearing in Eq. (10) with the energies of the corresponding subsystems. As such, the GMBE presented below will not be *derived* based on any systematic approximations to the supersystem Hamiltonian, but merely *motivated*. It is left to the numerical calculations in Sec. III to validate these arguments.

From this point of view, a fragmentation algorithm is simply a prescription for partitioning the nuclei into N subsets (some of which may intersect) that we denote $F_\alpha \equiv F_\alpha^{(1)}$, where $\alpha = 1, \ldots, N$. More generally, the notation $F_\beta^{(n)}$, where $\beta = 1, \ldots, {}_NC_n$, will indicate an n-mer constructed from the union of n distinct fragments. Dimers are constructed as unions of monomers, which we might variously indicate as

$$F^{(2)}_{F_\alpha \cup F_\beta} = F_\alpha \cup F_\beta = F^{(2)}_{\alpha\cup\beta}. \tag{11}$$

We emphasize that this dimer contains only one copy of each nucleus, even in the case of intersecting fragments, which is consistent with the set-theoretical notation that we employ. In some cases a more compact notation will be used, in which a dimer is denoted simply as $F_\gamma^{(2)}$, where $\gamma = 1, \ldots, {}_NC_2$ indexes the unique choices of α and β in Eq. (11). A similar notation will be used for higher-order n-mers.

As an example of this notation, consider the fragmentation scheme suggested in Fig. 1(c), and let the kth group be denoted as G_k. The first fragment in this diagram is a union of three different groups, $F_1^{(1)} = F^{(1)}_{G_1\cup G_2\cup G_3}$. The first dimer consists of a union of fragments 1 and 2: $F_1^{(2)} = F_1 \cup F_2$.

In the case of intersecting fragments, one may encounter n-mers that are subsets of other n-mers. As an example, consider why $F_1 \cup F_2$ is not listed amongst the possible dimers in Fig. 1(b). The dimer $F_1 \cup F_2$ includes the nuclei in groups G_1, G_2, and G_3, however, this is subset of the groups that are included in the dimer $F_1^{(2)}$, which is labeled as "dimer 1" in Fig. 1(b). Consider the system constructed from the union of $F_1 \cup F_2$ and $F_1^{(2)}$. An intersection-corrected energy for this system is obtained by computing the energies of $F_1 \cup F_2$ and of $F_1^{(2)}$, separately, and then subtracting the energy of their mutual intersection. The resulting intersection-corrected energy is

$$\begin{aligned} \mathcal{E} &= E^{(2)}_{F_1\cup F_2} + E^{(2)}_{F_1} - E^{(2)}_{(F_1\cup F_2)\cap F_1} \\ &= E^{(2)}_{F_1\cup F_2} + E^{(2)}_{F_1} - E^{(2)}_{F_1\cup F_2} \\ &= E^{(2)}_{F_1}. \end{aligned} \tag{12}$$

This example demonstrates that, computationally speaking, we need not consider any n-mer that is a subset of another n-mer, because PIE, as we apply it here, will lead to cancellation. From the standpoint of formal theory, inclusion of these subset n-mers poses no problem, because the net effect is to add zero.

2. Energy expression

To obtain the GMBE energy expression, let us proceed by means of an example based on Fig. 1(c). This panel illustrates a case of the m-body energy expression in Eq. (7) with $m = 2$ and $N = 3$. As such, we may immediately write down an approximation for the ground-state energy:

$$E \approx E^{(2)}_{F_1\cup F_2} + E^{(2)}_{F_1\cup F_3} + E^{(2)}_{F_2\cup F_3} - E^{(1)}_{F_1} - E^{(1)}_{F_2} - E^{(1)}_{F_3}. \tag{13}$$

However, because the fragments do not intersect in this particular case [see Fig. 1(c)], we have (for example)

$$E^{(1)}_{F_1} = E^{(2)}_{(F_1\cup F_2)\cap(F_1\cup F_3)}. \tag{14}$$

Furthermore, since $F_1 \cap F_2 \cap F_3 = \emptyset$ we could write $E^{(2)}_{F_1\cap F_2\cap F_3} = 0$. Exploiting these identities, we can rewrite Eq. (13) in an equivalent way:

$$\begin{aligned} E \approx\ & E^{(2)}_{F_1\cup F_2} + E^{(2)}_{F_1\cup F_3} + E^{(2)}_{F_2\cup F_3} - E^{(2)}_{(F_1\cup F_2)\cap(F_1\cup F_3)} \\ & - E^{(2)}_{(F_1\cup F_2)\cap(F_2\cup F_3)} - E^{(2)}_{(F_1\cup F_3)\cap(F_2\cup F_3)} \\ & + E^{(2)}_{(F_1\cup F_2)\cap(F_1\cup F_3)\cap(F_2\cup F_3)}. \end{aligned} \tag{15}$$

Comparing this expression to Eq. (8) suggests that Eq. (15) has the form of a summation (over all unique pairs of dimers) of intersection-corrected two-body energies. By careful analysis of Eq. (7), it becomes apparent this is possible for arbitrary N, in the case of non-intersecting fragments.

Although the argument above can be generalized to larger m, due to the factorial increase in the number of terms it is easier to pursue another line of thinking. To this end, consider Fig. 1(d) in which we have defined a set of ${}_NC_2$ "auxiliary" monomers, which are precisely the dimers from Fig. 1(c). By way of notation, let us denote the auxiliary monomers as $\widetilde{F}_\alpha \equiv \widetilde{F}_\alpha^{(1)}$ in order to distinguish them from the original monomers, $F_\alpha^{(1)}$. Unlike the original monomers, the auxiliary monomers *do* intersect, and thus far we know only one way to approximate the supersystem energy for intersecting monomers, namely, Eq. (8). Applying this equation to the particular set of auxiliary monomers in Fig. 1(d), one obtains

$$E \approx E^{(1)}_{\widetilde{F}_1} + E^{(1)}_{\widetilde{F}_2} + E^{(1)}_{\widetilde{F}_3} - E^{(1)}_{\widetilde{F}_1\cap\widetilde{F}_2} - E^{(1)}_{\widetilde{F}_1\cap\widetilde{F}_3} - E^{(1)}_{\widetilde{F}_2\cap\widetilde{F}_3} + E^{(1)}_{\widetilde{F}_1\cap\widetilde{F}_2\cap\widetilde{F}_3}. \tag{16}$$

This is identical to the energy expression in Eq. (15), once the identities of the fragments is recognized.

The procedure in the preceding paragraph can be generalized. Start from a set of non-intersecting fragments. At order m in the GMBE, we define a set of ${}_NC_m$ auxiliary monomers, each of which is identical to an m-mer formed from the non-intersecting fragments. The auxiliary monomers *do* intersect, and we therefore approximate the energy using Eq. (8). Finally, by realizing that the energy computed for these auxiliary monomers must be equal to that computed for the m-mers from which they arose, we obtain the m-body approximation to the total energy within the GMBE:

$$E^{(m)} = \sum_{\alpha=1}^{{}_NC_m} \mathcal{E}_\alpha^{(m)}, \tag{17}$$

where

$$\mathcal{E}_\alpha^{(m)} = E_\alpha^{(m)} - \sum_{\substack{\beta \\ (\beta>\alpha)}}^{{}_NC_m} E^{(m)}_{F_\alpha\cap F_\beta} + \sum_{\substack{\beta,\gamma \\ (\gamma>\beta>\alpha)}}^{{}_NC_m-1} E^{(m)}_{F_\alpha\cap F_\beta\cap F_\gamma} - \cdots + (-1)^{{}_NC_m-\alpha} E^{(m)}_{F_\alpha\cap F_{\alpha+1}\cap\cdots\cap F_{{}_NC_m}}. \tag{18}$$

In other words, the m-body approximation $E \approx E^{(m)}$ is a sum of intersection-corrected energies for the various m-mers constructed using a given fragmentation scheme.

Previously, we suggested that the GMBE follows the spirit of Eq. (7), a point on which we now elaborate. For any truncation order, m, we may compute an approximate energy $E^{(m)}$ as the sum of the energies of the ${}_NC_m$ distinct m-mers, so long as we take care not to double count any interactions. We ensure no double-counting occurs by appealing to PIE, as applied to the set of nuclei. Equation (7) can be interpreted similarly: it states that the m-body approximation to the energy is given by the sum of the m-mer energies, less a linear combination of the $(m-1)$-mer energies, the $(m-2)$-mer energies and so on, down to monomer energies. These terms need to be included so as to cancel any double-counting, but in the special case of non-intersecting monomers all intersections are readily evaluated in terms of monomers or unions of monomers. Furthermore, Eq. (17) reduces to Eq. (7) if the monomers do not intersect.

A useful feature of the traditional MBE, Eq. (6), is that one may check the convergence of the n-body approximation to the supersystem energy based on whether the $(n+1)$-body correction is negligible or not. This same sort of comparison is also possible for the GMBE. However, while one might anticipate that the terms $E^{(n)}$ in the traditional MBE will get smaller as n increases, it is not clear whether the same will be true of the GMBE. A second distinction is that once $E^{(n)}$ has been computed using the traditional MBE, the only new information that is needed to compute $E^{(n+1)}$ is the energy of each $(n+1)$-mer, of which there are ${}_NC_{n+1}$. In the case of the GMBE, however, the calculation of $E^{(n+1)}$ may also require the energies of some additional intersections that were not required to compute $E^{(n)}$.

E. Unified view of existing fragment methods

Having introduced the GMBE, our second goal is to define the concept of "fragment-based approach" in an elemental fashion, similar to the "molecules in molecules" (MIM) idea[8] but taking into account the more general energy expression derived above. The actual separation is to some extent semantic, but we find that four elements are sufficient to specify each such approach:

(1) a fragmentation method,
(2) a capping method,
(3) an embedding method, and
(4) the number of layers.

In Ref. 8, the capping method was included as part of the definition of the fragmentation method, but separating the two is useful for classifying some existing fragmentation approaches, such as the *molecular fractionation with conjugate caps* and related methods.[36–39] The "number of layers" in our list corresponds to the "MIM level" in Ref. 8, and although all of our calculations in Sec. III use only a single layer, we include this element for the sake of completeness as it is necessary for specifying multi-layer fragment methods.[8,18,19,22,27] (In the multi-layer case, the first three elements in our list would need to be specified for each layer.) By "embedding method," we mean an algorithm by means of which an exact or (more often) approximate electrostatic potential for the supersystem is added to each fragment electronic structure calculation.[40] The most common embedding schemes use atom-centered point charges to represent the other fragments; such procedures are discussed in more detail in Sec. II F.

The elemental scheme outlined above allows us to classify, and thus compare, a great many seemingly disparate fragment-based methods, and here we explore some examples that are relevant to the calculations presented in Sec. III. We have already mentioned the SMF method of Collins and co-workers;[24,33–35] in fact, three different fragmentation schemes are suggested in Ref. 24 ("levels one, two, and three" in the language of that paper), which differ in the number of

covalent bonds allowed between atoms in the same fragment. For the purpose of notation, let us denote these three approaches as SMF1, SMF2, and SMF3. The same capping method is used in each case, and all three methods employ only a single layer of theory. No embedding was employed in the original version of these methods,[24,33] although later a distributed-multipole[52] embedding was considered, along with terms intended to model dispersion interactions between non-bonded fragments.[34,41] The latter terms are not considered here, and the SMF1 calculations presented in Sec. III simply use the SMF1 fragmentation scheme, with or without an electronic embedding that is described in Sec. II F.

In SMF1, fragments are constructed from all possible pairs of covalently bonded groups. (In our implementation, this relies on either a user-defined connectivity or a default cutoff of 2.0 Å to define covalent bonds.) The fragments in Fig. 1(b) were constructed according to this algorithm. Specifically, we start with G_1 and form fragments $G_1 \cup G_i$ with any group G_i that is covalently bonded to G_1, in this case, G_2. We then proceed to G_2 and form all unique fragments $G_2 \cup G_i$, etc. The SMF2 and SMF3 fragmentation algorithms are similar except that groups connected by two or three covalent bonds, respectively, are included within a fragment. All three SMF approaches use the same capping method: after severing a covalent bond between atoms located at $\mathbf{r}_1$ and $\mathbf{r}_2$, a hydrogen atom is placed at position $\mathbf{r}_{\rm cap}$ defined by

$$\mathbf{r}_{\rm cap} = \mathbf{r}_1 + \left(\frac{R_1 + R_{\rm H}}{R_1 + R_2}\right)(\mathbf{r}_2 - \mathbf{r}_1), \tag{19}$$

where R_x is the atomic radius of atom x. We will call this the "SMF capping method."

The GEBF approach of Li and co-workers[26,31,32] is another relevant example that can largely be viewed as an alternative fragmentation method. The GEBF fragmentation method starts with G_1 and creates a fragment that includes G_1 and all other groups that lie within some specified distance, ξ, of the atoms in G_1. (We take $\xi = 3.0$ Å, as in Ref. 26.) The GEBF approach uses the same capping method as in SMF, and also uses an electrostatic embedding based on charges derived from natural population analysis.[42] The embedding charges, which could in principle be converged self-consistently with the fragment self-consistent field (SCF) wave functions, by means of a "dual SCF" procedure,[43,44] are found to be converged, or very nearly so, after only one iteration.[26]

Unfortunately, the charge-embedding procedure that is used in the GEBF method leads to non-variational SCF wave functions, because the embedding potential is simply grafted onto the SCF equations without proper account for how the embedding charges vary with respect to changes in the SCF wave function.[43–45] As a result, the derivatives $\delta E_{\rm SCF}/\delta\phi_i^A$, where ϕ_i^A represents the ith occupied molecular orbital on molecule A, are not zero, even if they are iterated to fully self-consistent convergence with the fragment SCF wave functions. As such, correct analytical gradients ought to require the solution of coupled-perturbed equations—even at the SCF level—whose dimension equals the dimension of the entire (super)system. Although we are not the first to make this observation,[46,47] this point is neither discussed in any of the GEBF papers,[26,31,32] nor in the majority of other papers where the embedding charges are iterated to self-consistency.[34,35,48] It implies that putative analytic gradients published for some of these methods are formally incorrect,[31,32,49] despite having been used in the past for geometry optimizations and frequency calculations.[50,51] (In a similar vein, correct analytic gradients for the fragment molecular orbital (FMO) method[1,53–55] were reported only recently,[47] following several "approximate" versions of the FMO gradient.[56,57])

TABLE I. Elemental classification of various fragment-based methods.

Method	Fragment method	Capping method	Embedding method	No. of layers
SMF1[a]	SMF1(1)	SMF	None	1
SMF2[a]	SMF2(1)	SMF	None	1
SMF3[a]	SMF3(1)	SMF	Mone	1
GEBF[b]	GEBF(1)	SMF	XPol[c]	1
SMF1(2)[d]	SMF1(2)	None	None	1
EE-SMF1(2)[d]	SMF1(2)	None	EE-MB-b[e]	1
GEBF(1)[d]	GEBF(1)	None	None	1
EE-GEBF(1)[d]	GEBF(1)	None	EE-MB-b[e]	1
GEBF(2)[d]	GEBF(2)	None	None	1
EE-GEBF(2)[d]	GEBF(2)	None	EE-MB-b[e]	1

[a]Introduced in Ref. 24.
[b]Introduced in Ref. 26.
[c]Embedding method from Ref. 43, introduced in this work for self-consistent GEBF calculations.
[d]New in this work.
[e]Embedding method from Ref. 13.

Next, let us discuss how the MBE fits into the unified, elemental framework suggested here. As discussed in Sec. II D, the MBE can be viewed as a systematic procedure for creating ever-larger monomers, and as such we view the MBE as a part of the fragmentation method. The *generalized* MBE is used to define the energy formula, whether or not the fragments intersect. In view of this, we will adopt the notation "XYZ(n)" to mean that fragmentation method XYZ has been used in conjunction with an n-body truncation of the GMBE; only the $n = 1$ and $n = 2$ cases are considered here.

Using this nomenclature, the method known in the literature as GEBF (Refs. 26, 31, and 32) is here denoted GEBF(1), since it uses the one-body energy formula defined in Eqs. (8) and (9) [or, equivalently, the GMBE in Eq. (17), truncated at $m = 1$]. The GEBF(2) method, which is introduced here for the first time, fragments the system in the same way but evaluates the energy using the two-body version of the GMBE.[58] Table I summarizes how we categorize various approaches on the basis of the elemental classification scheme suggested above.[59] Further examples of this classification scheme are discussed in the supplementary material,[61] where we discuss the fragment molecular orbital method,[53–55] the kernel energy method,[62–65] the hybrid many-body interaction method,[15–17] and various ONIOM-like QM:QM methods,[8,18–23] in addition to methods already mentioned explicitly above.

F. Electrostatic embedding

We alluded above to the fact that the GEBF approach[26,31,32] to obtaining self-consistent embedding

charges does not preserve the variational nature of the fragment SCF wave functions, and therefore complicates the formulation of analytic gradients.[49] The reason is that this (and other[34,35,48]) self-consistent charge-embedding procedures simply graft a charge–density interaction term onto the SCF energy expression, without modifying the accompanying Fock matrix, and therefore without consideration for how the embedding charges vary with respect to changes in the SCF wave function. This can be remedied by explicitly incorporating these variations into the fragment Fock matrices,[43,44] in what has come to be called the *explicit polarization* (XPol) method.[43,66,67] The charge derivatives $\partial q_i/\partial P_{\mu\nu}$ that are required to construct the extra terms in the Fock matrix have been reported for Mulliken charges, Löwdin charges, and "ChElPG" charges[69,70] that are fit to reproduce the molecular electrostatic potential,[44,45] and we find that the ChElPG charges are the most stable.[44] The XPol method has recently been suggested as a means to incorporate electrostatic embedding into the MBE in a variational fashion,[68] which we shall pursue in some of the calculations in Sec. III.

Most of our calculations, however, utilize the charge embedding scheme introduced by Dahlke and Truhlar[13] in the context of what they term the *electrostatically embedded many-body* (EE-MB) method. Two different versions were introduced in Ref. 13, and we use "version b" (EE-MB-b), in which gas-phase monomer calculations are used to determine Mulliken charges for each monomer. The gas-phase charges are then used as fixed embedding charges for the subsequent fragment calculations. At first glance this seems rather crude, although EE-MB results are found to be surprisingly insensitive to the precise details of the embedding charges.[13,71] For some systems (e.g., zwitterionic glycine in water), self-consistency is found to have a more significant effect,[72] and we will make a limited exploration of self-consistent embedding charges for the $F^-(H_2O)_{10}$ system in Sec. III C 2. Our main focus in this work, however, is a comparison of MBE- and GMBE-based methods.

The EE-MB-b charge embedding has not previously been defined for methods that allow intersecting fragments, and its extension to intersecting fragments is ambiguous because atoms contained within intersections might have different charges in different fragments. To resolve this ambiguity, we define the embedding charge for a particular atom to be the average of its charge in all fragments. This definition is a temporary workaround that is not without problems (as discussed in Sec. III), and we intend to consider alternatives in future work. Nevertheless, it works surprisingly well for many of the systems considered here. Methods denoted EE-XYZ(n) include this version of electrostatic embedding.

III. NUMERICAL RESULTS

A. Computational details

We will consider numerical applications to $(H_2O)_N$ and $F^-(H_2O)_{10}$ clusters described at either the Hartree-Fock (HF) or B3LYP levels of theory. The 6-31+(d,2p) basis set is used for all of the B3LYP calculations, whereas HF calculations use 6-31G(d) for $(H_2O)_N$ and 6-31+G(d) for $F^-(H_2O)_{10}$. Water cluster geometries ranging from $N = 3$ to $N = 10$ were obtained from Ref. 21, and geometries for a set of $F^-(H_2O)_{10}$ isomers were generated by means of molecular dynamics with the AMOEBA force field.[73] The $F^-(H_2O)_{10}$ cluster geometries are available in the supplementary material.[61]

Fragment-based calculations are designed to replicate the results of a supersystem electronic structure calculation, at reduced cost. Ideally, owing to the embarrassingly parallelizable nature of the approach, the largest individual electronic structure calculation should represent the computational bottleneck, assuming that sufficient processors are available. (The situation is more complicated for methods where embedding charges are determined self-consistently.) However, for calculations based on the *generalized* MBE, the cost of determining all of the mutual intersections between fragments may actually become prohibitive. In the Appendix, we prove that the cost of fragmentation based on PIE scales exponentially with the number of fragments. Thus, if the GMBE is to be a useful approach for large molecules, clever fragmentation algorithms that avoid this bottleneck will need to be developed. We are currently pursuing such approaches, with promising preliminary results as discussed in the Appendix. Here, our focus is on accuracy, in order to first establish that GMBE-based approaches are worth pursuing at all.

Of the methods introduced in Table I, we do not consider the one-body methods SMF1(1) or EE-SMF1(1), because the fragments in these cases are limited to a single H_2O molecule or F^- ion, and thus these methods are nearly devoid of intermolecular interactions. The GEBF(1) method also truncates the GMBE at the one-body level, but employs larger fragments and is therefore worth considering. For the systems considered here, the SMF1(2) method is equivalent to a two-body expansion with non-intersecting fragments, which has been considered previously for water clusters,[13] and the EE-SMF1(2) approach is, for $(H_2O)_N$, completely equivalent to the EE-MB approach used in Ref. 13. These calculations provide a useful point of comparison for GEBF(2) results, which are considered here for the first time.

Fragmentation is performed with an in-house program that generates input files for the Q-CHEM electronic structure program.[74] The raw energetic data can be found in the supplementary material.[61] As a concise summary and useful companion for the discussion below, Table II summarizes the statistical errors for each method, where the error is defined with respect to a supersystem calculation. Table III summarizes these same statistical errors on a per-monomer basis.

B. Water clusters

1. Absolute energies

We first consider how accurately the fragment methods reproduce the total energy of a supersystem calculation. Figure 2 plots the unsigned errors resulting from each of six different approaches. For the least accurate methods, the errors emerge in a hierarchal manner so that we can make a general statement that the accuracy increases in the order SMF1(2) < GEBF(1) < EE-SMF1(2). Each of the other

TABLE II. Mean signed error (MSE) and mean absolute error (MAE), both in kcal/mol, as obtained using various fragment methods.

System	Method	Type of error	No embedding			Mulliken embedding[a]		
			SMF1(2)	GEBF(1)	GEBF(2)	SMF1(2)	GEBF(1)	GEBF(2)
Absolute	HF	MSE	17.83	4.39	0.00	2.04	0.69	0.00
energies,	HF	MAE	17.83	5.59	0.01	2.04	0.72	0.02
$(H_2O)_N$[b]	B3LYP	MSE	12.12	3.56	0.17	1.93	0.34	− 0.01
	B3LYP	MAE	12.12	4.06	0.47	1.93	0.41	0.03
Relative	HF	MSE	− 0.12	6.27	− 0.01	0.15	0.46	0.05
energies,	HF	MAE	1.47	6.65	0.01	0.58	0.55	0.05
$(H_2O)_N$[b]	B3LYP	MSE	− 0.70	4.97	1.65	− 0.05	0.33	0.05
	B3LYP	MAE	1.23	5.88	1.65	0.37	0.48	0.06
Relative	HF	MSE	− 0.22	− 2.36	0.37	0.09	− 2.77	0.09
energies,	HF	MAE	1.46	6.84	0.46	0.19	3.30	0.09
$F^-(H_2O)_{10}$	B3LYP	MSE	− 0.70	4.97	1.65	− 0.05	0.33	0.05
	B3LYP	MAE	2.51	6.36	1.07	0.52	2.57	0.13

[a]EE-MB-b embedding (Ref. 13) using gas-phase Mulliken charges.
[b]$N \leq 10$.

three methods—GEBF(2), EE-GEBF(1), and EE-GEBF(2)—exhibits errors not substantially larger than 1 kcal/mol.

The relative accuracy of certain methods is readily explained in terms of fragment size. The SMF1(1) fragments consist of individual water molecules, and it follows that the fragments in SMF1(2) are water dimers. In fact, for these particular systems, SMF1(2) is equivalent to a traditional two-body cluster expansion. We anticipate large many-body polarization effects in $(H_2O)_N$ clusters (e.g., 9–13 kcal/mol in the hexamer[75]), and indeed many of the SMF1(2) errors are larger than 10 kcal/mol. The GEBF fragmentation approach, on the other hand, leads to fragments consisting of three or four water molecules, whose intermolecular interactions are therefore incorporated even at the one-body level, and errors are reduced to the 1–10 kcal/mol range for GEBF(1) calculations. We note that GEBF(1) is *not* equivalent to SMF1(3) or SMF1(4), where the fragments are trimers and tetramers, respectively, because the GEBF(1) method omits three- and four-body interactions between water molecules more distant than $\xi = 3.0$ Å. These would be included in SMF1(3) and SMF1(4) calculations.

We find that EE-SMF1(2) is actually more accurate than GEBF(1), despite the fact that the former approach does not include any *explicit* three-body interactions at all. Three-body and higher-order effects are included in EE-SMF1(2) *implicitly* (and approximately), via the embedding charges, whereas GEBF(1) neglects all many-body effects beyond those that arise explicitly from the presence of three or four H_2O molecules per fragment. These observations are especially noteworthy in view of the reduced fragment size in EE-SMF1(2) relative to GEBF(1).

In order to make contact with previous literature, we should note that the SMF1(2) method, as applied to water clusters, is equivalent to standard two-body application of the MBE; Dahlke and Truhlar[13] have termed this the *many-body pairwise additive* (MB-PA) approach. EE-SMF1(2) calculations for $(H_2O)_N$, with the embedding scheme used here, are equivalent to the EE-MB-PA method of Ref. 13. We should also note that our implementation of GEBF(1) differs slightly from the method originally implemented by Li *et al.*,[26] insofar as we use fixed, gas-phase Mulliken charges for the electrostatic embedding, whereas in Ref. 26

TABLE III. Summary of errors in absolute energies per monomer (in kcal/mol), using various fragment methods.

System	Method	Type of error	No embedding			Mulliken embedding[a]		
			SMF1(2)	GEBF(1)	GEBF(2)	SMF1(2)	GEBF(1)	GEBF(2)
Absolute	HF	MSE	2.04	0.49	0.00	0.25	0.07	0.00
energies,	HF	MAE	2.04	0.58	0.00	0.25	0.08	0.00
$(H_2O)_N$[b]	B3LYP	MSE	1.75	0.50	0.03	0.27	0.05	0.00
	B3LYP	MAE	1.75	0.56	0.06	0.27	0.06	0.00
Absolute	HF	MSE	− 1.45	0.59	0.04	0.10	− 0.95	0.01
energies,	HF	MAE	1.45	0.74	0.05	0.10	0.95	0.01
$F^-(H_2O)_{10}$	B3LYP	MSE	− 2.21	0.56	0.08	− 0.10	− 0.64	0.00
	B3LYP	MAE	2.21	0.71	0.08	0.10	0.74	0.01
Absolute	HF	MSE	4.87	3.80	2.69	0.45	0.22	0.13
energies,	HF	MAE	4.87	3.80	2.69	0.45	0.22	0.13
$(H_2O)_{57}$	B3LYP	MSE	3.74	2.95	2.07	− 0.36	− 0.40	− 0.31
	B3LYP	MAE	3.74	2.95	2.07	0.36	0.40	0.31

[a]EE-MB-b embedding (Ref. 13) using gas-phase Mulliken charges.
[b]$N \leq 10$.

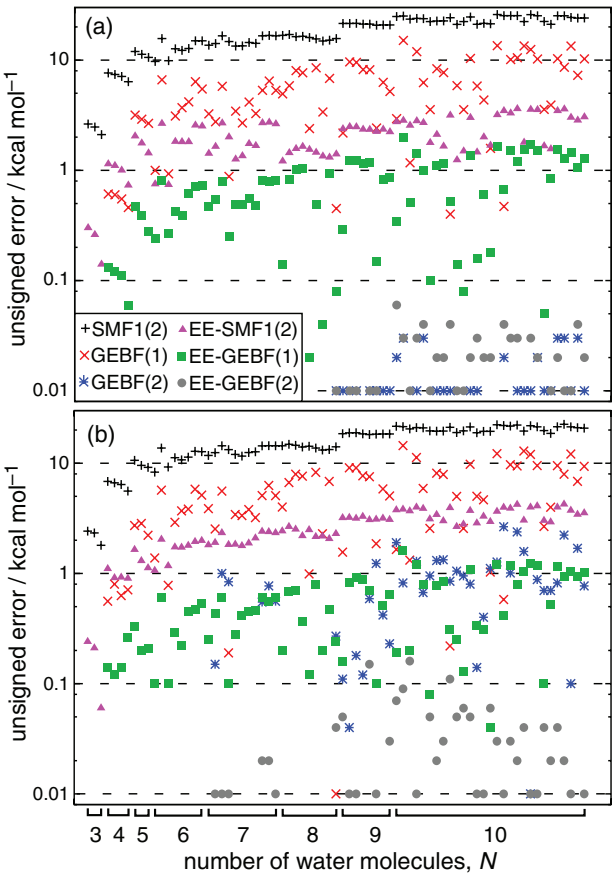

FIG. 2. Total unsigned errors (plotted on a logarithmic scale) in fragment-based calculations for $(H_2O)_N$ clusters at (a) the HF/6-31G(d) and (b) the B3LYP/6-31+G(d,2p) level.

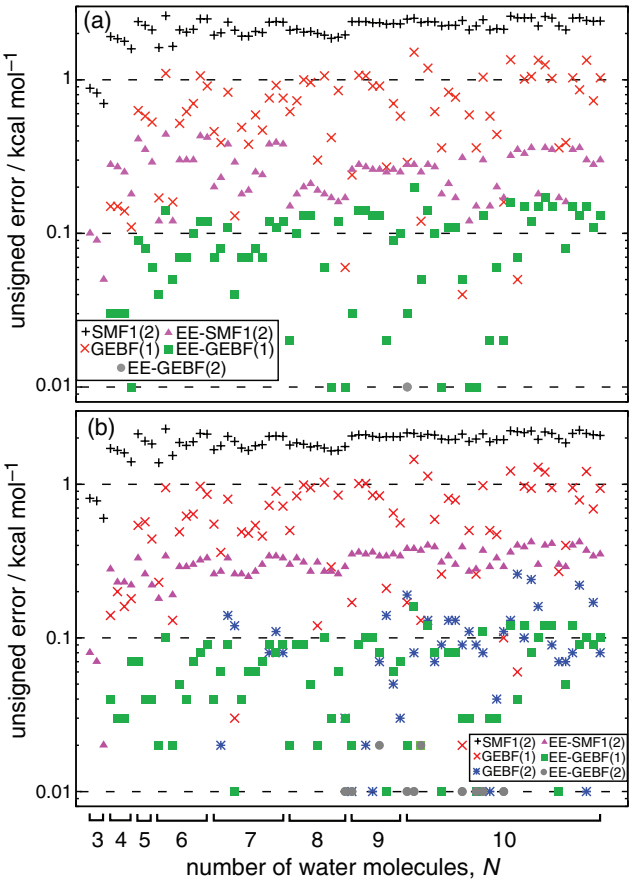

FIG. 3. Total unsigned errors per monomer, plotted on a logarithmic scale, in fragment-based calculations for $(H_2O)_N$ clusters at (a) the HF/6-31G(d) and (b) the B3LYP/6-31+G(d,2p) level.

the charges were obtained from natural population analysis[42] and were iterated toward self-consistency. Interestingly, for the $(H_3O^+)_5(HO^-)_5(H_2O)_{22}$ system considered in Ref. 26, self-consistent iteration modifies the embedding charges by only $\sim 0.01e$, so for the rather simple test systems examined in this work, the lack of self-consistency may not be a major concern.

In contrast, the GEBF(2) and EE-GEBF(2) methods are introduced here for the first time, which would not have been possible except for the formulation of the GMBE in Eq. (17) that extends the MBE to intersecting monomers. These are the first two-body calculations to exploit intersecting monomers,[76] and it is apparent from Fig. 2 that extending the GEBF method to dimers has the desired result. Comparing GEBF(1) and GEBF(2), we see an increase in accuracy of one or two orders of magnitude when the dimer terms are included. A similar increase in accuracy is observed in comparing EE-GEBF(1) to EE-GEBF(2) and indeed we will see that the intersecting-dimer approaches generally outperform the intersecting-monomer approaches.

As pointed out by Beran,[15] for non-covalent clusters one expects that the total error to be an extensive quantity in fragment-based calculations. The absolute errors per monomer, which are intensive, are plotted in Fig. 3 and the corresponding error statistics are listed in Table III. For the SMF1(2) and EE-SMF1(2) methods, we obtain MAEs of about 2 kcal/mol/H_2O and 0.2 kcal/mol/H_2O, respectively. (As a check of our implementation, we note that these values are in good agreement with the statistical errors reported by Dahlke and Truhlar for the same systems, using the equivalent MB-PA and EE-MB-PA methods.[13]) The GEBF(2) and EE-GEBF(2) methods prove to be much more accurate, with MAEs and MSEs of <0.01 kcal/mol/H_2O. We should note that data points with errors less than 0.1 kcal/mol are not shown in either Fig. 2 or Fig. 3, since the range of the data is such that it would be awkward to plot all of them on a single set of axes, even using a logarithmic scale. The absence of a data point for a particular method thus indicates that the error is basically negligible. (The raw data can, however, be found in the supplementary material.[61])

2. Relative energies

The error statistics for absolute energies (which translate directly into errors in the cluster binding energies) are quite promising, but it is important to consider relative conformational energies as well. For the purpose of this comparison, we set $E = 0$ for each cluster size based on whichever structure is lowest in energy for the supersystem calculation, meaning that the fragment methods may afford negative relative energies if the lowest-energy isomer is predicted incorrectly. The isomer whose energy is set to zero is not included in computing error statistics.

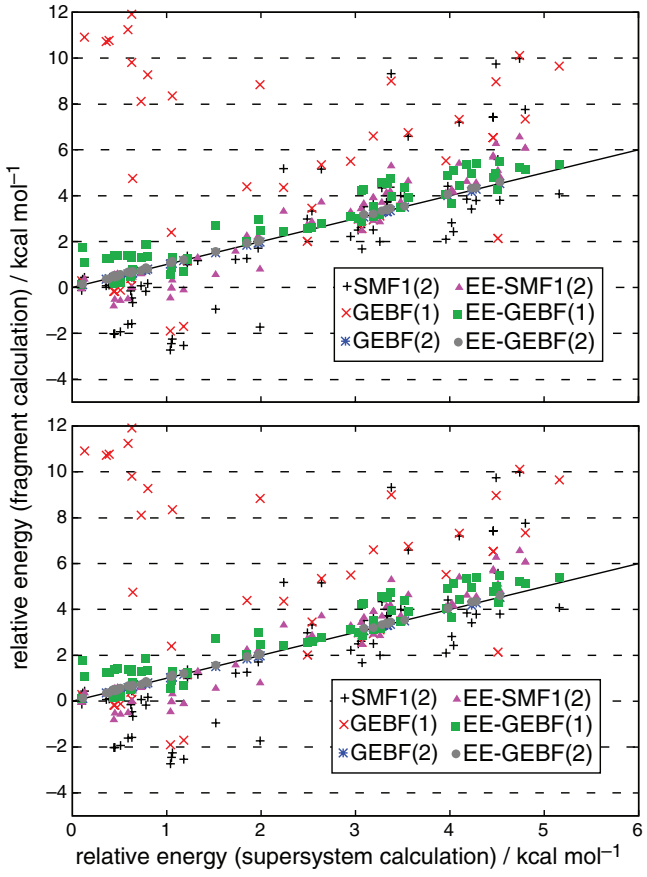

FIG. 4. Relative energies for $(H_2O)_N$ clusters predicted by fragment-based methods, as compared exact (supersystem) results, at (a) the HF/6-31G(d) level and (b) the B3LYP/6-31+G(d,2p) level. The oblique solid line corresponds to exact agreement with a supersystem calculation.

Figure 4 plots the relative energy as predicted by the fragment methods against the correct (i.e., supersystem) relative energy. The GEBF(1) results are quite poor, with errors that approach 20 kcal/mol in some cases. [In fact, several GEBF(1) data points lie outside of the range plotted in Fig. 4, but to avoid further compressing the more interesting data, these points are omitted. The complete data set is provided in the supplementary material.[61]] This observation is particularly interesting because it means that SMF1(2) performs *better* than GEBF(1) for relative energies, despite performing *worse* for absolute energies. The explanation lies in the fact that all of the SMF1(2) absolute energy errors have the same sign (as can be inferred from the fact that the MAE and the MSE in Table II are identical), whereas GEBF(1) exhibits both positive and negative errors in the absolute energies. The GEBF(1) errors lie erratically around the supersystem result, leading to larger errors in *relative* energies.

The water decamer provides an illustrative example. In this case, GEBF(1) *overstabilizes* the minimum-energy isomer by about 3 kcal/mol at the HF/6-31G(d) level but *understabilizes* the so-called "PP2" isomer[21] by 15 kcal/mol, for a total MAE of 18 kcal/mol. The SMF1(2) approach understabilizes both structures by about 25 kcal/mol, so that the error in the absolute electronic energy is significantly larger for either isomer, as compared to GEBF(1) results, but the SMF1(2) error in the relative energies is <1 kcal/mol.

Much of the literature on fragment-based quantum chemistry methods has focused on errors in absolute energies with respect to supersystem calculations, with water clusters being a popular test system. Relative conformational energies have been considered far less frequently, leaving us with little precedent as to the magnitudes of errors that we might expect. Tschumper and co-workers[19] have considered a series of water clusters with the intent of benchmarking how well an ONIOM-like "QM:QM" approach reproduces high-level *ab initio* results. The QM:QM approach is equivalent to a "level two" MIM expansion,[8] in which a lower level of theory (MP2/cc-pVTZ in this case) is applied to the full system and corrected by means of a three-body expansion at a higher level of theory [CCSD(T)/aug-cc-pVTZ]. Amongst the calculations presented in Ref. 19, of particular interest are a series of five $(H_2O)_{16}$ isomers, for which a MAE of 0.1 kcal/mol is reported for the relative isomer energies. This is in good agreement with results presented here for two-body methods.

Pruitt *et al.*[77] have considered the relative energies of various isomers of the open-shell $OH(H_2O)_5$ cluster within the FMO approach,[1,54] which merits some explanation. The FMO method employs user-defined fragments and frozen-orbital caps whenever covalent bonds are severed,[54] and both a two-body truncation of the MBE ("FMO2") and a three-body truncation ("FMO3") have been introduced. For clusters such as $(H_2O)_N$ or $OH(H_2O)_5$, FMO calculations have typically employed single-molecule fragments, in which case FMO2 is the same as EE-SMF1(2), except that FMO2 uses self-consistent (albeit non-variational) Mulliken embedding charges, whereas our EE-SMF1(2) charges are fixed at gas-phase values.

FMO2 calculations for six different isomers of $OH(H_2O)_5$, with fragment calculations performed at the ROMP2/aug-cc-pVTZ level, are found to afford a MAE of 1.7 kcal/mol in the relative isomer energies.[77] This may be compared to the MAEs of 0.4–0.6 kcal/mol reported in Table II for EE-SMF1(2) calculations of $(H_2O)_N$ relative energies at the HF and B3LYP levels. One should not read too much into this comparison, given that the systems in question are different, yet the significantly smaller errors observed in the EE-SMF1(2) calculations suggest that the lack of self-consistency in the EE-SMF1(2) embedding charges is perhaps not the largest source of error in these calculations. Rather, the two-body truncation, and the use of single-molecule fragments, seem to be more important than the intimate details of the charge-embedding scheme. This supposition is supported, to some extent, by the fact that three-body FMO3 calculations reduce the MAE in the $OH(H_2O)_5$ relative energies to 0.3 kcal/mol.[77] In view of this, it is promising that EE-GEBF(2) calculations for $(H_2O)_N$ clusters exhibit MAEs of only 0.05 kcal/mol.

3. Larger water clusters

The GEBF(2) and EE-GEBF(2) results presented above seem quite promising, but one might object that because the GEBF(2) fragmentation algorithm results in 3–4 H_2O molecules per fragment, some of the fragments constitute

a significant fraction of the total cluster size, which might make the results appear more favorable than they would be in larger systems. To investigate this possibility, we next consider a $(H_2O)_{57}$ cluster, in order to ascertain whether GEBF(2) and EE-GEBF(2) remain the most accurate approaches when the resulting dimers no longer comprise a majority of the molecule. Geometries for this cluster were extracted from a molecular dynamics simulation and are available in the supplementary material.[61]

In order to reduce the number of dimers that we need to consider, for this particular system we have employed two cutoffs. For SMF1(2) calculations we consider only those pairs of monomers that are within 3.0 Å of each other. Because the GEBF(1) monomers are larger, we reduced this cutoff to 1.0 Å for GEBF(1) calculations, which has the effect that dimers are created only from monomers that intersect. Admittedly, these cutoffs are considerably more aggressive than what has been used in the literature to date, e.g., Dahlke and Truhlar[22] utilize a 5–6 Å cutoff for water clusters. We justify our choice by the simple fact that it affords reasonable accuracy. In future work, the convergence with respect to the dimer cutoff distance should be investigated.

Table III lists the MSEs and MAEs for these clusters on a per-molecule basis, and the trends mirror what we observe in smaller clusters. Of the non-embedded approaches, GEBF(2) performs the best and is about 1 kcal/mol more accurate than GEBF(1), and 2 kcal/mol more accurate than SMF1(2). Electrostatic embedding increases the accuracy by about an order of magnitude, and EE-GEBF(2) is the most accurate embedded method. Relative to the results in smaller water clusters, we do observe a notable increase in the error per monomer at both the GEBF(1) and GEBF(2) levels, with or without electrostatic embedding, although the errors remain small ($\leq$0.4 kcal/mol, with embedding). The important point is that for $(H_2O)_{57}$, the GEBF(2) dimers no longer encompass the majority of the cluster and we expect these results to be more typical of the errors that one can expect when using GEBF(2) in large clusters, i.e., we are probing the intrinsic accuracy of the method in these calculations.

To place this level of error in context, we note that FMO2 results reported for a single isomer of $(H_2O)_{64}$, performed using B3LYP/6-31+G* and B3LYP/6-31++G** with two H_2O molecules per fragment, were larger than 0.7 kcal/mol/H_2O.[78] At the FMO3 level, the same setup results in errors less than 0.1 kcal/mol/H_2O.[78] In a recent study,[79] the accuracy of the SMF and FMO methods was compared for water clusters, defining water molecules within 2.3 Å of one another to be "bonded" for the purposes of applying the SMF3 fragmentation method. Proceeding in this way, the accuracy of SMF3 and FMO3 was found to be similar. A more detailed comparison awaits improvements to our fragmentation procedure that will allow for systematic tests of the thresholding procedures discussed in the Appendix.

C. Fluoride–water clusters

As compared to neat water clusters, hydrated ions may represent more challenging systems due to the greater degree of polarization and the large ion–water interaction. Indeed, FMO calculations on large $Na^+(H_2O)_N$ clusters have shown that two-body (FMO2) calculations yield very poor approximations to the total energy, with errors greater than 65 kcal/mol even with as many as 31 H_2O molecules included in the same fragment as the cation, and ~100 kcal/mol when only six water molecules are included with Na^+.[80] (FMO3 calculations perform much better, although errors remain on the order of 2–6 kcal/mol, even with a very large central fragment.[80]) Hydrated anions are likely to be even more challenging owing to the greater extent of charge delocalization associated with the ion, and here we perform tests on a set of $F^-(H_2O)_{10}$ using one- and two-body GMBE methods.

1. Fixed-charge embedding

Figure 5 plots errors in the total energy per monomer for a set of ten $F^-(H_2O)_{10}$ isomers, using the same fixed-charge embedding procedure that was used for the water clusters. For the most part, the trends that we observe are the same as those observed for water clusters: SMF1(2) performs the worst and EE-GEBF(2) performs the best, electrostatic embedding generally improves the accuracy of the results, and the use of intersecting monomers generally improves the accuracy as well.

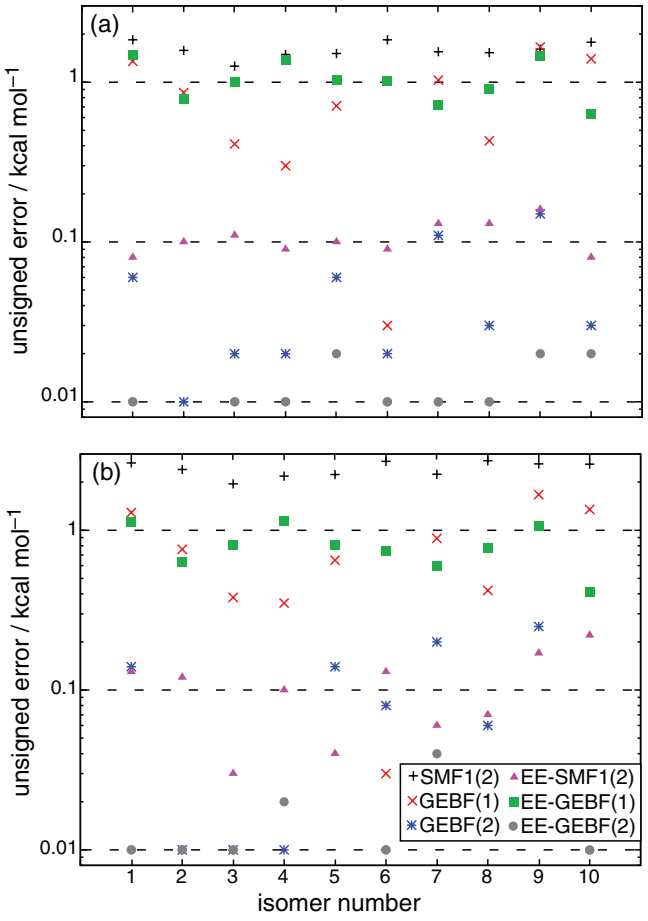

FIG. 5. Unsigned error in the total electronic energy per water monomer (plotted on a logarithmic scale) for a set of ten $F^-(H_2O)_{10}$ cluster isomers. Calculations were performed at (a) the HF/6-31+G(d) and (b) the B3LYP/6-31+G(d,2p) levels of theory.

One anomaly stands out, however. For neutral water clusters, EE-GEBF(1) was a significant (factor of ten) improvement over GEBF(1), yet for these fluoride–water clusters both methods exhibit comparable accuracies of ∼1 kcal/mol. This may be due to over-polarization brought about by using intersecting monomers. Suppose that water molecule *A* belongs to the same monomer as the fluoride ion. In such a case, one would expect *A*'s electron density to be significantly distorted relative to what it would be when *A* appears in another, charge-neutral fragment. As a result of this asymmetry, the embedding point charges are averages over two very different electronic environments. (Recall from Sec. II F that for intersecting monomers we use fragment-averaged point charges for the electrostatic embedding.) In principle, the same error is present in EE-GEBF(2) calculations, though perhaps less pronounced owing to increased dimer size, and in fact EE-GEBF(2) is significantly more accurate for $F^-(H_2O)_{10}$ relative energies, as compared to the other methods considered here. Nevertheless, these observations point to the need to explore alternative ways to compute embedding charges in the case of intersecting monomers.

Relative energies of the fluoride–water clusters are plotted versus supersystem results in Fig. 6. Again we see that GEBF(1) is the least accurate method for relative energies, whereas EE-GEBF(2) is the most accurate. The main point of interest for these figures is that the errors obtained using EE-GEBF(1) and EE-GEBF(2) are an order of magnitude larger than what was observed in application of the same methods to $(H_2O)_N$ clusters. We suspect that this is once again a deficiency of the embedding charges, and points to the need to explore alternate, self-consistent embedding schemes.

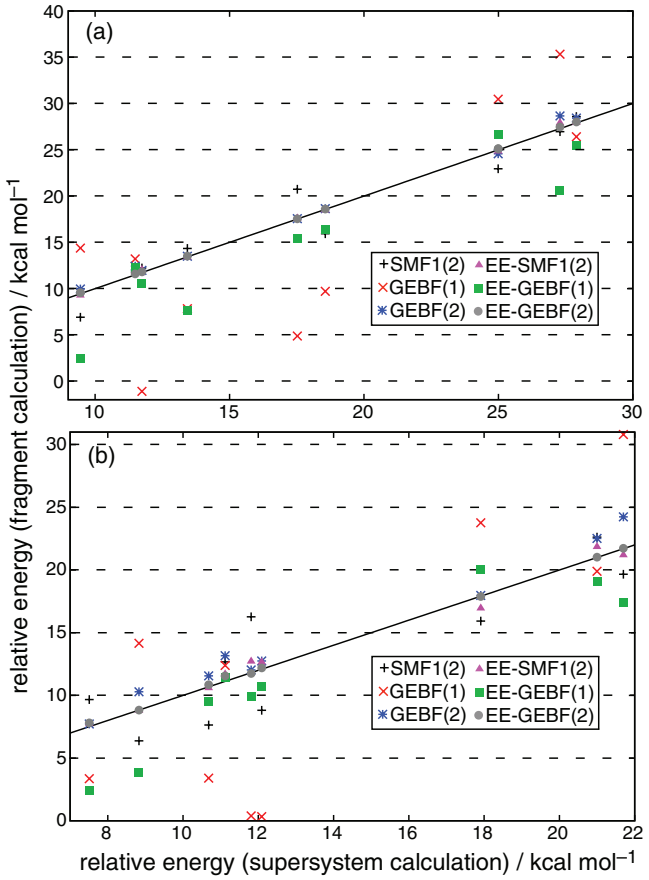

FIG. 6. Relative energies for isomers of $F^-(H_2O)_{10}$ as predicted by various fragment methods at (a) the HF/6-31+G(d) and (b) the B3LYP/6-31+G(d,2p) level of theory. The oblique solid line indicates exact agreement with the supersystem calculation.

2. Self-consistent XPol embedding

As a preliminary example of one such self-consistent charge embedding, we consider the use of XPol/ChElPG embedding charges. As noted in Sec. II F, a naïve implementation of self-consistency will cause the total energy to be non-variational.[49] This can be avoided by the use of XPol embedding charges, as was recently suggested in the context of the MBE.[68]

As a simple example to illustrate the procedure, consider a conventional two-body approximation to the energy of the trimer *IJK*, where *I*, *J*, and *K* are non-intersecting fragments. Following Eqs. (1) and (2), let us write this approximation in the following way:

$$E_{IJK} \approx E^{(1)}_{Ijk} + E^{(1)}_{iJk} + E^{(1)}_{ijK} + \Delta E^{(2)}_{IJk} + \Delta E^{(2)}_{IjK} + \Delta E^{(2)}_{iJK}. \tag{20}$$

Capitalized indices in this expression imply that the indexed fragment is treated at the SCF level, while fragments with lower-case indices are represented by embedding charges. All three one-body terms can be extracted from a single XPol calculation on *IJK*, whereas each two-body calculation requires a separate XPol calculation in which one of the fragments is a dimer. For example, the $\Delta E^{(2)}_{IJk}$ term would be computed using an XPol calculation involving two fragments: *IJ* and *K*. In that particular calculation, SCF equations on *K* must be iterated to convergence even though it is ultimately only *IJ*'s energy that is extracted from the calculation, which introduces additional computational complexity as compared to the more naïve self-consistent procedures discussed above, but the number of additional iterations is minimal. (Even when starting from isolated, gas-phase initial-guess wave functions, the XPol procedure typically converges in ≤4 loops over monomers.)

Error statistics for the GEBF(1) and GEBF(2) methods with XPol embedding, as applied to $F^-(H_2O)_{10}$, are listed in Table IV. For comparison, we also tabulate the statistical errors using fixed, gas-phase ChElPG embedding charges (analogous to the "EE-MB-b" embedding used above but with ChElPG charges replacing Mulliken charges). For the GEBF(1) method, XPol embedding does afford an increase in accuracy for both absolute and relative energies as compared to earlier results using fixed, fragment-averaged embedding charges, and the same is true if we obtain these fixed charges using ChElPG. This suggests that at least part of the problem with the earlier EE-GEBF(1) results is indeed related to erratic polarization caused by the fragmented-averaged charges. On the other hand, the EE-GEBF(2)/ChElPG results for relative isomer energies are significantly *worse* when the charges are iterated to self-consistency (cf. the last two columns in Table IV).

TABLE IV. Statistical errors in EE-GEBF(n) calculations for $F^-(H_2O)_{10}$ isomers using ChElPG embedding charges, in units of kcal/mol/H_2O. Results are compared for fixed gas-phase ChElPG embedding charges and for charges that are converged self-consistently using the XPol procedure. All ChElPG calculations use a grid spacing $\Delta x = 1.0$ Å.

		Absolute energies				Relative energies			
	Type	GEBF(1)		GEBF(2)		GEBF(1)		GEBF(2)	
Method	of error	Fixed	XPol	Fixed	XPol	Fixed	XPol	Fixed	XPol
HF	MSE	− 0.76	− 0.34	0.01	0.00	− 2.45	− 2.10	0.08	1.09
HF	MAE	0.76	0.34	0.01	0.06	2.82	1.86	0.08	1.13
B3LYP	MSE	− 0.46	− 0.03	0.10	0.08	− 1.55	− 1.30	0.36	1.41
B3LYP	MAE	0.46	0.12	0.10	0.12	2.29	1.60	0.36	1.68

For the calculations reported in Table IV, we used a fairly coarse ChElPG grid spacing of 1.0 Å, as this was sufficient to provide reasonable results in previous XPol/ChElPG calculations.[45] [It is also sufficient to provide very accurate GEBF(2) results when gas-phase ChElPG embedding charges are used, as the results in Table IV will attest.] However, the 1.0 Å grid spacing engenders a fairly serious loss of rotational invariance, which went unnoticed in our previous work,[44,45] probably because the weighted least-squares procedure that we use to compute the ChElPG charges[45] ensures that the charges are smooth functions of the nuclear coordinates. Provided that one works only in the molecule-fixed coordinate frame, the lack of rotational invariance may therefore go completely unnoticed. In the present context, however, simply re-ordering the fragments in the Q-CHEM input file (which amounts to rotating the molecule-fixed frame with respect to the laboratory frame) may change the energy by $\sim 10^{-4}$ E_h.

To examine this issue further, we have performed EE-SMF1(2) calculations using a finer grid ($\Delta x = 0.3$ Å), and Table V compares these results to those obtained using $\Delta x = 1.0$ Å. The fine grid reduces the errors in absolute energies only slightly (by about 0.2 kcal/mol/H_2O), relative to results obtained with the coarser grid, but significantly reduces the errors in the relative energies (by about a factor of two for the MAEs and a factor of ten for the MSEs). However, the fine grid also significantly increases the cost of these calculations, to the point that we have not attempted GEBF(n) calculations with the finer grid, as the number of electronic structure calculations is much larger for these methods.

One puzzling aspect of the data in Table V is the fact that results obtained using gas-phase ChElPG embedding charges remain more accurate than the self-consistent, XPol-embedded results. This is especially true for absolute energies, where the fixed-charge results exhibit errors of $\leq$0.1 kcal/mol/H_2O, even when the coarse grid is used, whereas XPol-embedded results with the fine grid exhibit errors of 0.7–0.8 kcal/mol/H_2O. For *relative* energies, the XPol-embedded results are only slightly worse than those obtained using gas-phase embedding charges, which makes us wonder whether the problem may once again stem from lack of rotational invariance. We are currently working to implement ChElPG charges using sparse, atom-centered grids, which will significantly reduce the computational overhead such that more systematic tests can be performed. This approach should also reduce the magnitude of the rotational invariance errors.[81,82]

IV. CONCLUSIONS

We have introduced a GMBE for fragment-based quantum chemistry, which extends the traditional MBE to the case where fragments may share some nuclei in common. Application of the GMBE, truncated at some n-body level of approximation, provides a systematic means to approach the exact supersystem energy, analogous to how the MBE is applied in the case of non-intersecting fragments. The GMBE, which reduces to the traditional MBE in the case of non-intersecting fragments, provides a universal energy

TABLE V. Statistical errors in EE-SMF1(2) calculations for $F^-(H_2O)_{10}$ isomers using ChElPG embedding charges, in units of kcal/mol/H_2O. Results are compared for fixed gas-phase ChElPG embedding charges and for charges that are converged self-consistently using the XPol procedure.

		Absolute energies			Relative energies		
	Type	Fixed	XPol charges		Fixed	XPol charges	
Method	of error	charges[a]	Coarse grid[a]	Fine grid[b]	charges[a]	Coarse grid[a]	Fine grid[b]
HF	MSE	0.10	0.83	0.66	0.14	− 1.28	− 0.15
HF	MAE	0.10	0.83	0.66	0.30	1.12	0.64
B3LYP	MSE	0.00	0.99	0.78	0.02	− 1.59	− 0.29
B3LYP	MAE	0.03	0.99	0.78	0.37	1.61	0.75

[a]Grid spacing $\Delta x = 1.0$ Å.
[b]Grid spacing $\Delta x = 0.3$ Å.

expression for fragment-based methods, which are therefore differentiated by their fragmentation, capping, and embedding procedures, but not by the formula that is used to compute the energy.

This formulation provides a unified view of several fragment-based methods that have been proposed previously, and suggests that it is possible to create a number of novel fragment-based methods simply by combining elements from existing approaches in new ways. One of these new ways, namely, a two-body extension of the previously-reported GEBF method[26,31,32] (which, in fact, is based on the same energy expression as the CG-MTA approach[25,29,30]) is reported here for the first time, and appears to be quite promising.

Numerical results for $(H_2O)_N$ and $F^-(H_2O)_{10}$ clusters indicate that methods based on intersecting fragments are more accurate, for both absolute and relative energies, than are methods that utilize non-intersecting fragments, when the GMBE is truncated at the two-body level. Notably, this remains true even in large clusters such as $(H_2O)_{57}$, where all of the fragments are small as compared to the size of the overall system. Although electrostatic embedding in most cases significantly improves the accuracy of results based on the GMBE (as seen in many previous studies using the traditional MBE), for the $F^-(H_2O)_{10}$ we find that this need not be the case. The reason probably lies in the use of fixed embedding charges, which was done here in order to make contact with previous methods in the literature, and points to the need to develop self-consistent charge embedding schemes for use with the GMBE.

At present, the primary drawback that limits applications of the GMBE is the steep cost of computing all possible mutual intersections between different fragments, which is necessary once the fragments are allowed to intersect. Efforts to reduce this cost by means of thresholding procedures are currently underway in our group, and we expect that improved fragmentation algorithms will facilitate systematic tests of GMBE-based fragment methods, in the near future.

ACKNOWLEDGMENTS

This work was supported by a National Science Foundation CAREER award (CHE-0748448) and calculations were performed at the Ohio Supercomputer Center under Project No. PAS-0291. J.M.H. is an Alfred P. Sloan Foundation Fellow and a Camille Dreyfus Teacher-Scholar.

APPENDIX: COMPUTATIONAL SCALING

Here, we discuss the computational scaling of fragmentation based on PIE, and some aspects of our fragmentation algorithm. Let n_I denote the number of elements in fragment I. In order to deduce the scaling of PIE, imagine that we start with fragment I and compute $I \cap J$. The cost of this calculation should scale asymptotically as $(n_I + n_J)\log(n_I + n_J)$, because it could be performed by sorting the $n_I + n_J$ nuclear indices into an ordered list and checking for repeated indices. For simplicity, consider a case where all of the fragments have the same size, n. Then the cost to determine $I \cap J$ is $\mathcal{O}(n \log n)$. By storing the elements of $I \cap J$, one may readily compute $I \cap J \cap K$ by concatenating the list of indices in $I \cap J$ with the list of indices from K, and then performing a sort. Since $|I \cap J| \leq n$, we can assume that the cost of computing $I \cap J \cap K$ is $\mathcal{O}(n \log n)$ at worst, and by induction this is true of higher-order intersections ($I \cap J \cap K \cap L$, etc.) as well.

If there are N fragments in total, then the number of intersections involving m fragments is ${}_NC_m$, so the total time (in the worst case) looks like

$$t \sim (n \log n) \sum_{m=2}^{N} \binom{N}{m}. \tag{A1}$$

The summation can be expressed in closed form if the lower limit is extended to $m = 0$, with the result that

$$t \sim (n \log n)(2^N - N - 1). \tag{A2}$$

For large N, we therefore have

$$t \sim 2^N (n \log n), \tag{A3}$$

where n is indicative of the typical number of nuclei in a fragment, and N is the total number of fragments.

In the worst-case scenario, Eq. (A3) demonstrates that the cost of applying PIE scales exponentially with the number of fragments. However, this argument makes two unrealistic assumptions: first, that all intersections are nonempty; and second, that each intersection to be searched takes a roughly constant number of operations ($n\log n$). As such, Eq. (A3) should be treated as an upper bound to the actual cost of fragmentation.

In practice, we can use a backtracking algorithm to reduce the cost considerably, such that evaluation of the intersections is quite efficient in cases where a large fraction of the intersections are empty. As an example to illustrate this point, we take the protein TM1081 that was considered in a recent study by Collins.[35] This protein contains 2048 atoms, corresponding to 689 groups and 699 fragments according to the SMF1(1) algorithm. Despite the seemingly intractable factor of $2^{699} \approx 2.6 \times 10^{210}$ that appears in Eq. (A3), our algorithm requires only about 3 min, running on a laptop, to determine the groups, fragments, intersections, and caps, and to generate the necessary Q-CHEM input files.

Nevertheless, in dense three-dimensional systems such as water clusters, backtracking alone is insufficient to enable us to evaluate all terms suggested by the GEBF(2) method for a system such as $(H_2O)_{57}$. To perform the $(H_2O)_{57}$ calculations reported here we had to resort to a distance-based threshold in which we only consider dimers formed from fragments within 1 Å of one another, which effectively limits dimer formation to intersecting fragments. Table VI compares the number of distinct electronic structure input files that are generated for various fragmentation schemes as applied to $(H_2O)_{10}$, where we compute every single term that appears in the one- or two-body GMBE, and also for $(H_2O)_{57}$, where the 1 Å threshold for dimer formation is applied. If all terms in the energy expression are enumerated, then the GEBF(2) approach results in a *significantly* larger number of electronic structure calculations, but distance-based thresholding can reduce this number substantially. In fact, at the GEBF(1) level, the $(H_2O)_{57}$ calculation with thresholds actually requires *fewer* independent

TABLE VI. Number of distinct electronic structure calculations required by various fragment-based approaches in two different systems. For $(H_2O)_{10}$, all terms in the one- or two-body GMBE are included, but for SMF1(2) and GEBF(2) calculations in $(H_2O)_{57}$, dimers more than 1 Å apart are neglected.

Method	$(H_2O)_{10}$	$(H_2O)_{57}$
SMF1(2)	55	111
GEBF(1)	38	15
GEBF(2)	484	628

electronic structure calculations than does a calculation for $(H_2O)_{10}$ with no thresholds.

For geometry optimizations or molecular dynamics simulations, the use of thresholding will require a careful implementation that utilizes switching functions to attenuate a particular dimer's contribution to the energy as its constituent monomers move apart. Development of such techniques is presently underway in our group.

[1] M. S. Gordon, D. G. Fedorov, S. R. Pruitt, and L. V. Slipchenko, Chem. Rev. **112**, 632 (2011).
[2] W. Kohn, Phys. Rev. Lett. **76**, 3168 (1996).
[3] E. Prodan and W. Kohn, Proc. Natl. Acad. Sci. U.S.A. **102**, 11635 (2005).
[4] H. Stoll and H. Preuß, Theor. Chim. Acta **46**, 11 (1977).
[5] J. C. White and E. R. Davidson, J. Chem. Phys. **93**, 8029 (1990).
[6] H. Stoll, Phys. Rev. B **46**, 6700 (1992).
[7] E. Suárez, N. Díaz, and D. Suárez, J. Chem. Theory Comput. **5**, 1667 (2009).
[8] N. J. Mayhall and K. Raghavachari, J. Chem. Theory Comput. **7**, 1336 (2011).
[9] J. Gauss, "Molecular properties," *Modern Methods and Algorithms of Quantum Chemistry*, NIC Series Vol. 3, 2nd ed., edited by J. Grotendorst (John von Neumann Institute for Computing, Jülich, 2000), pp. 541–592.
[10] M. Svensson, S. Humbel, R. D. J. Froese, T. Matsubara, S. Sieber, and K. Morokuma, J. Phys. Chem. **100**, 19357 (1996).
[11] S. Dapprich, I. Komáromi, K. S. Byun, K. Morokuma, and M. J. Frisch, J. Mol. Struct.: THEOCHEM **461–462**, 1 (1999).
[12] W. J. Hehre, L. Radom, P. v. R. Schleyer, and J. A. Pople, *Ab Initio Molecular Orbital Theory* (Wiley, 1986).
[13] E. E. Dahlke and D. G. Truhlar, J. Chem. Theory Comput. **3**, 46 (2007).
[14] S. Wen, K. Nanda, Y. Huang, and G. J. O. Beran, Phys. Chem. Chem. Phys. **14**, 7579 (2012).
[15] G. J. O. Beran, J. Chem. Phys. **130**, 164115 (2009).
[16] A. Sebetci and G. J. O. Beran, J. Chem. Theory Comput. **6**, 155 (2010).
[17] G. J. O. Beran and K. Nanda, J. Phys. Chem. Lett. **1**, 3480 (2010).
[18] G. S. Tschumper, Chem. Phys. Lett. **427**, 185 (2006).
[19] D. M. Bates, J. R. Smith, T. Janowski, and G. S. Tschumper, J. Chem. Phys. **135**, 044123 (2011).
[20] A. M. Elsohly, C. L. Shaw, M. E. Guice, B. D. Smith, and G. S. Tschumper, Mol. Phys. **105**, 2777 (2007).
[21] D. M. Bates, J. R. Smith, and G. S. Tschumper, J. Chem. Theory Comput. **7**, 2753 (2011).
[22] E. E. Dahlke and D. G. Truhlar, J. Chem. Theory Comput. **3**, 1342 (2007).
[23] E. E. Dahlke, H. R. Leverentz, and D. G. Truhlar, J. Chem. Theory Comput. **4**, 33 (2008).
[24] V. Deev and M. A. Collins, J. Chem. Phys. **122**, 154102 (2005).
[25] V. Ganesh, R. K. Dongare, P. Balanarayan, and S. R. Gadre, J. Chem. Phys. **125**, 104109 (2006).
[26] W. Li, S. Li, and Y. Jiang, J. Phys. Chem. A **111**, 2193 (2007).
[27] B. W. Hopkins and G. S. Tschumper, Mol. Phys. **103**, 309 (2005).
[28] I. G. Kaplan, R. Santamaria, and O. Novaro, Mol. Phys. **84**, 105 (1995).
[29] A. P. Rahalkar, V. Ganesh, and S. R. Gadre, J. Chem. Phys. **129**, 234101 (2008).
[30] A. P. Rahalkar, M. Katouda, S. R. Gadre, and S. Nagase, J. Comput. Chem. **31**, 2405 (2010).
[31] S. Hua, W. Hua, and S. Li, J. Phys. Chem. A **114**, 8126 (2010).
[32] W. Li, W. Hua, T. Fang, and S. Li, "The energy-based fragmentation approach for ab initio calculations of large systems," in *Computational Methods for Large Systems: Electronic Structure Approaches for Biotechnology and Nanotechnology*, edited by J. R. Reimers (Wiley, Hoboken, NJ, 2011), pp. 227–258.
[33] M. A. Collins and V. A. Deev, J. Chem. Phys. **125**, 104104 (2006).
[34] M. A. Addicoat and M. A. Collins, J. Chem. Phys. **131**, 104103 (2009).
[35] M. A. Collins, Phys. Chem. Chem. Phys. **14**, 7744 (2012).
[36] D. W. Zhang and J. Z. H. Zhang, J. Chem. Phys. **119**, 3599 (2003).
[37] A. M. Gao, D. W. Zhang, J. Z. H. Zhang, and Y. Zhang, Chem. Phys. Lett. **394**, 293 (2004).
[38] S. Li, W. Li, and T. Fang, J. Am. Chem. Soc. **127**, 7215 (2005).
[39] N. Jiang, J. Ma, and Y. Jiang, J. Chem. Phys. **124**, 114112 (2006).
[40] Although the embedding point charges are present in each fragment electronic structure calculation, and therefore polarize the fragment wave functions, the self-energy (mutual Coulomb interaction) of these embedding charges should *not* be included in the fragment energy, as this amounts to overcounting of electron–electron interactions.
[41] J. M. Mullin, L. B. Roskop, S. R. Pruitt, M. A. Collins, and M. S. Gordon, J. Phys. Chem. A **113**, 10040 (2009).
[42] A. E. Reed, R. B. Weinstock, and F. Weinhold, J. Chem. Phys. **83**, 735 (1985).
[43] W. Xie, L. Song, D. G. Truhlar, and J. Gao, J. Chem. Phys. **128**, 234108 (2008).
[44] L. D. Jacobson and J. M. Herbert, J. Chem. Phys. **134**, 094118 (2011).
[45] J. M. Herbert, L. D. Jacobson, K. U. Lao, and M. A. Rohrdanz, Phys. Chem. Chem. Phys. **14**, 7679 (2012).
[46] S. Hirata, J. Chem. Phys. **129**, 204104 (2008).
[47] T. Nagata, K. Brorsen, D. G. Fedorov, K. Kitaura, and M. S. Gordon, J. Chem. Phys. **134**, 124115 (2011).
[48] H.-A. Le, H.-J. Tan, J. F. Ouyang, and R. P. A. Bettens, J. Chem. Theory Comput. **8**, 469 (2012).
[49] The GEBF analytic gradient expressions that appear in Refs. 31 and 32 are formally incorrect because they do not include the response terms that arise from the embedding charges, which are present even for an infinitesimal perturbation since $\delta E_{\rm SCF}/\delta\phi_i^A \neq 0$ at convergence. These incorrect gradient expressions were subsequently used for geometry optimizations and harmonic frequency calculations.[32,50,51] In some cases, results compared favorably to supersystem calculations. For large systems, however, the "errors" reported in Ref. 32 are actually differences in GEBF calculations using two different fragment sizes, rather than differences with respect to supersystem calculations. The magnitude of the errors due to neglect of the response terms therefore remains to be determined. A self-consistent embedding procedure that has been introduced in the context of SMF calculations,[34,35] based on distributed multipole analysis,[52] is also non-variational, for the same reason.
[50] W. Hua, T. Fang, W. Li, J.-G. Yu, and S. Li, J. Phys. Chem. A **112**, 10864 (2008).
[51] Z. Yang, S. Hua, W. Hua, and S. Li, J. Phys. Chem. A **114**, 9253 (2010).
[52] A. J. Stone, J. Chem. Theory Comput. **1**, 1128 (2005).
[53] K. Kitaura, E. Ikeo, T. Asada, T. Nakano, and M. Uebayasi, Chem. Phys. Lett. **313**, 701 (1999).
[54] D. G. Fedorov and K. Kitaura, J. Phys. Chem. A **111**, 6904 (2007).
[55] D. G. Fedorov and K. Kitaura, "Theoretical background of the fragment molecular orbital (FMO) method and its implementation in GAMESS," in *The Fragment Molecular Orbital Method: Practical Applications to Large Molecular Systems*, edited by D. G. Fedorov and K. Kitaura (CRC, Boca Raton, FL, 2009), pp. 5–36.
[56] K. Kitaura, S.-I. Sugiki, T. Nakano, Y. Komeiji, and M. Uebayasi, Chem. Phys. Lett. **336**, 163 (2001).
[57] T. Nagata, D. G. Fedorov, and K. Kitaura, Chem. Phys. Lett. **492**, 302 (2010).
[58] The notation GEBF(n) is used in Ref. 32 in a different (and unrelated) sense.
[59] We omit a detailed discussion of group formation. Most fragment-based methods construct groups to ensure that fragments do not cut across multiple bonds, although exceptions have been considered in order to treat extended π systems.[60] The systems treated here do not contain multiple bonds so this issue does not arise.
[60] S. D. Yeole and S. R. Gadre, J. Chem. Phys. **132**, 094102 (2010).
[61] See supplementary material at http://dx.doi.org/10.1063/1.4742816 for a discussion of the elemental classification of various fragment-based approaches, for the raw data used to compute error statistics, and for Cartesian coordinates of the $F^-(H_2O)_{10}$ and $(H_2O)_{57}$ systems.
[62] L. Huang, L. Massa, and J. Karle, Int. J. Quantum Chem. **103**, 808 (2004).

[63]L. Huang, L. Massa, and J. Karle, Proc. Natl. Acad. Sci. U.S.A. **105**, 1849 (2008).
[64]S. N. Weiss, L. Huang, and L. Massa, J. Comput. Chem. **31**, 2889 (2010).
[65]L. Huang, H. J. Bohorquez, C. F. Matta, and L. Massa, Int. J. Quantum Chem. **111**, 4150 (2011).
[66]An early version of the XPol method[67] did *not* include the Fock matrix corrections that are necessary to make the fragment SCF wave functions variational. However, we use the term "XPol" exclusively to mean the variational formulation that was first reported in Ref. 43.
[67]W. Xie and J. Gao, J. Chem. Theory Comput. **3**, 1890 (2007).
[68]J. Gao and Y. Wang, J. Chem. Phys. **136**, 071101 (2012).
[69]L. E. Chirlian and M. M. Francl, J. Comput. Chem. **8**, 894 (1987).
[70]C. M. Breneman and K. B. Wiberg, J. Comput. Chem. **11**, 361 (1990).
[71]H. R. Leverentz and D. G. Truhlar, J. Chem. Theory Comput. **5**, 1573 (2009).
[72]M. Kamiya, S. Hirata, and M. Valiev, J. Chem. Phys. **128**, 074103 (2008).
[73]J. W. Ponder, C. Wu, P. Ren, V. S. Pande, J. D. Chodera, M. J. Schnieders, I. Haque, D. L. Mobley, D. S. Lambrecht, R. A. DiStasio, Jr., M. Head-Gordon, G. N. I. Clark, M. E. Johnson, and T. Head-Gordon, J. Phys. Chem. B **114**, 2549 (2010).
[74]Y. Shao, L. Fusti-Molnar, Y. Jung, J. Kussmann, C. Ochsenfeld, S. T. Brown, A. T. B. Gilbert, L. V. Slipchenko, S. V. Levchenko, D. P. O'Neill, R. A. DiStasio, Jr., R. C. Lochan, T. Wang, G. J. O. Beran, N. A. Besley, J. M. Herbert, C. Y. Lin, T. Van Voorhis, S. H. Chien, A. Sodt, R. P. Steele, V. A. Rassolov, P. E. Maslen, P. P. Korambath, R. D. Adamson, B. Austin, J. Baker, E. F. C. Byrd, H. Dachsel, R. J. Doerksen, A. Dreuw, B. D. Dunietz, A. D. Dutoi, T. R. Furlani, S. R. Gwaltney, A. Heyden, S. Hirata, C.-P. Hsu, G. Kedziora, R. Z. Khalliulin, P. Klunzinger, A. M. Lee, M. S. Lee, W. Liang, I. Lotan, N. Nair, B. Peters, E. I. Proynov, P. A. Pieniazek, Y. M. Rhee, J. Ritchie, E. Rosta, C. D. Sherrill, A. C. Simmonett, J. E. Subotnik, H. L. Woodcock III, W. Zhang, A. T. Bell, A. K. Chakraborty, D. M. Chipman, F. J. Keil, A. Warshel, W. J. Hehre, H. F. Schaefer III, J. Kong, A. I. Krylov, P. M. W. Gill, and M. Head-Gordon, Phys. Chem. Chem. Phys. **8**, 3172 (2006).
[75]Y. Chen and H. Li, J. Phys. Chem. A **114**, 11719 (2010).
[76]From a certain point of view, intersecting dimers were considered in the SMF calculations of Ref. 24, insofar as pairs of groups that were not covalently bonded were explicitly incorporated into the set of fragments. The important distinction is that these were pairs of *groups*, not pairs of *monomers*, and thus they constitute additional fragments rather than dimers.
[77]S. R. Pruitt, D. G. Fedorov, K. Kitaura, and M. S. Gordon, J. Chem. Theory Comput. **6**, 1 (2010).
[78]D. G. Fedorov and K. Kitaura, Chem. Phys. Lett. **389**, 129 (2004).
[79]S. R. Pruitt, M. A. Addicoat, M. A. Collins, and M. S. Gordon, Phys. Chem. Chem. Phys. **14**, 7752 (2012).
[80]T. Fujita, K. Fukuzawa, Y. Mochizuki, T. Nakano, and S. Tanaka, Chem. Phys. Lett. **478**, 295 (2009).
[81]U. C. Singh and P. A. Kollman, J. Comput. Chem. **5**, 129 (1984).
[82]B. H. Besler, K. M. Merz, Jr., and P. A. Kollman, J. Comput. Chem. **11**, 431 (1990).